SARS-CoV-2 variants'-Alpha, Delta, and Omicron D614G and P681R/H mutations impact virus entry, fusion, and infectivity

Ritika Khatri
Translational Health Science and Technology Institute
Gazala Siddqui
Translational Health Science and Technology Institute
Srikanth Sadhu
Translational Health Science and Technology Institute
Vikas Maithil
Translational Health Science and Technology Institute
Preeti Vishwakarma
Translational Health Science and Technology Institute https://orcid.org/0000-0001-8530-4860
Bharat Lohiya
Translational Health Science and Technology Institute
Abhishek Goswami
Translational Health Science and Technology Institute
Shubbir Ahmed
Translational Health Science and Technology Institute
Amit Awasthi
Translational Health Science and Technology Institute https://orcid.org/0000-0002-2563-1971
Sweety Samal (sweety.samal@thsti.res.in)
Translational Health Science and Technology Institute

Article

Keywords:

Posted Date: February 1st, 2022

DOI: https://doi.org/10.21203/rs.3.rs-1310197/v1

Abstract

SARS-CoV-2 variants acquire mutations to survive within the host and evade immunity. In addition to harboring D614G mutation in spike domain, P681R/H mutation at the junction of the S1/S2 furin cleavage site, is found to be the key mutation in variants of concerns (VoC); Alpha, Delta, and Omicron (B.1.1.519). The impact of these acquired mutations on entry, transmissibility, and infectivity of SARS-CoV2 VoC is not clearly identified. Here, using the spike-based pseudovirus, Delta and D614G+P681R synthetic mutants showed a significant increase in the pseudovirus entry, fusion, and infectivity. In contrast, Omicron spike-based pseudovirus and a synthetic P681H mutant showed preferential hACE2-mediated virus entry over TMPRSS2, less fusion, and highly susceptible to Cathepsin L inhibitor. Taken together, these results indicate while the Delta variant utilizes both ACE2 and TMPRSS2 mediated entry, thus causing systemic infection; Omicron has favored growth in ACE2 expressed cells thus mainly replicating in the upper respiratory tract.

Introduction

The severe acute respiratory coronavirus 2 (SARS-CoV-2) is a positive-sense, single stranded, enveloped, RNA virus which belongs to the Coronaviridae family, genus beta corona virus[1]. Since the emergence of SARS-CoV-2 pandemic in late 2019, the virus has been evolved, although the mutation rate of SARS-CoV-2 was found to be approximately 1.1 × 10-3 substitutions/site/year [2 3], which is slower than other important RNA viruses such as HIV-1 and Influenza [4]. However, certain SARS-CoV-2 Variants of Concerns (VoC) have emerged over the two years and few are found to be highly infectious and resulted in rapid spread to various regions of the world, thus causing the second (Alpha variant) and the third pandemic wave (Delta variant)[5]. In November 2021, another important VoC virus named as Omicron has emerged in South Africa, which then rapidly spread to many parts of the world and resulted in the fourth pandemic wave [6].

The first important variant was observed in May 2020 which consists of a single mutation, aspartic acid at 614 position to glycine mutation (D614G) in the spike protein and later on this D614G mutant has found to be highly infectious and adventitious for SARS-CoV-2 virus fitness [7]. The D416G virus infection resulted in high viral load in upper respiratory tract though the disease severity was not significantly altered as compared to ancestral Wuhan-1 strain [8]. Later on Alpha variant (B.1.1.7) was identified first in United Kingdom in September 2020 and declared as Variant of Concern [9]. The alpha variant has 17 mutations in the spike protein[10], the major RBD mutation N501Y have shown enhance binding to ACE2 and resulted in escape neutralization [11]. The B.1.1.7 Alpha variant also contains D614G and a cleavage site mutation P681H, which might facilitate increase virus entry to epithelial cells [12,13]. The third major pandemic wave was caused by Delta variant (B.1.617.2) in late 2020 in India and later on spread to all over the world in more than 90 countries [14]. The Delta variant caused severe disease, high replication in both upper and lower airway tract, enhanced syncytial formation, significant increase in virus entry and marked reduction in vaccine effectiveness [15–17], The Delta variant contains D614G and P681R mutation

at S1/S2 cleavage site respectively. Currently circulating Omicron variant contains ~33 mutations in spike protein and also harbors the D614G and P681H mutations as similar to Alpha variant. The new Omicron variant was found to be enhanced transmissibility but with milder symptoms [18]. Baric RS et.al have showed D614G mutation allows highly fit virus which can efficiently replicate in nasal airway thus could result in high transmission and more stable than the ancestral Wuhan-1 strain and the single mutation is associated with high infectivity as compared to ancestral virus [19].

SARS-CoV-2 virus mediates infection by binding of the envelop spike protein to cellular receptor hACE2, which is highly expressed on epithelial cells of the airway tract, lung and intestine [20,21] and in lower level in other major organs such as kidney, heart and male and female reproductive tract [22–25]. The binding of spike protein to ACE2 receptor facilitates conformational changes leading to proteolytic cleavage of spike protein at S1/S2 junction, and formation of activated spike protein. The cleavage of spike protein leads to exposure of fusion peptide that initiates the fusion process between viral-host cell membrane. Although the exact mechanism of SARS-CoV-2 virus entry and fusion is still intriguing, a large number of studies propose SARS-CoV-2 could enter host cell via two pathways i) Endocytic pathway, thus cleavage processing by Cathepsin L proteases inside late endosomes ii) Cell surface pathway which can activate spike protein at cell surface by cleaving through serine proteases TMPRSS2 [26,27]. The highly conserved cleavage site sequence plays an important role in allowing the SARS-CoV-2 virus entry and thus determining the infectivity and transmission. The SARS-CoV-2 virus evolutionary pathway suggests the presence of D614G along with P681R/H mutation might have a role in virus entry, fusion and transmission. To understand the role of these important mutations, we have utilized HIV-1/spike pseudovirus system to generate ancestral, D614G, Alpha, Delta, Omicron, single P681H mutant and D614G+P681R double mutant pseudoviruses. Here, we showed the double mutant D614G+P681R results in enhanced infectivity, fusion, syncytial and marked increase in virus entry through both ACE2 and TMPRSS2 route as similar to Delta virus, suggesting the presence of D614G and P681R mutations are sufficient for Delta variant to induce enhanced infectivity and pathogenicity. In contrast, the Omicron pseudovirus consisting of D614G and P681H mutation along with other mutations in spike protein, showed ACE2-dependent virus entry, low fusion and syncytial formation and reduced infectivity titer as compared to Delta variant. In the Omicron spike the proline 681-was mutated to Histidine instead of Arginine as seen in Delta. Our findings showed single P681H mutant phenotypically behave more similar to Alpha and Omicron variant. This single mutation P681H in the spike protein in the cleavage site might attributes towards the better fitness of Omicron virus on upper airway epithelium, thus leading to high transmission but lower pathogenicity.

Results

Pseudovirus variants of concerns and synthetic mutants' expression and cleavability

Site-directed mutagenesis was performed on the full-length wildtype ancestral Wuhan-1 spike protein to produce D614G, P681H and D614G+P681R double mutants to generate pseudoviruses. Alpha (B.1.1.7)

variant spike was generated in-house which consists of all the mutations in spike protein except the 69-70 deletion; the wild type parental Wuhan-1, Delta (B.1.617.2) and Omicron (B.1.1.529) spike variants were gene synthesized and the pseudoviruses were generated as described in Methods section (Fig.1a). All the spike mutants were well-expressed in BHK-21 transfected cells (Supplementary Fig.1). We further assessed the expression of the spike protein of all the variants and mutants on cell surface w.r.t wild type spike via flow cytometry in HEK293T mammalian cells. As compared to ancestral/wildtype spike protein, the expression of variants or mutants spike protein were found to be significantly increased (Supplementary Fig.2). We then analyzed the binding of surface expressed spike protein to soluble hACE2 by flow cytometry. The Delta, Omicron and synthetic D614G+P681R spike showed ~2-fold increase in the binding to soluble hACE2 (Fig1b). Earlier it has been shown that D614G mutation significantly alters the spike conformation, thus modulating the interaction with hACE2 receptor which in turn affects virus entry and infectivity [28]. The presence of D614G mutation present in the variants or mutant spike protein might have altered the conformation, thus modulating the binding to hACE2. However, in the single P681H mutant also, there was increase in binding to hACE2, which suggests this is a crucial mutation that could also alter the spike conformation. The other key mutations present in the Delta or Omicron variants might have effect in the spike conformation. Peacock P. Thomas et.al have recently shown introduction of Q498R in Alpha variant, which is also present in Omicron, increases binding to soluble hACE2 [29].

Next, we analyzed the cleavage of spike protein incorporated in pseudovirions at 24 and 48h post transfection. The concentrated pseudovirions were analyzed by Western blot and as shown in Fig.1c, except Alpha pseudovirus spike protein, rest all variants spikes were cleaved at 24h post transfection, whereas in case of Omicron, more pronounced cleavage was shown at 48h post transfection, where more distinct cleaved S2 band was seen at ~100kDa. The pseudoviruses were prepared in 293T cells which contains inherent furin like proteases. This suggests Alpha and Omicron pseudoviruses might have slow cleavage processing in presence of furin as compared to Delta pseudoviruses. A similar phenomenon was shown by Ueo. A et.al, where Mumps virus fusion was inefficiently cleaved when expressed in 293T cells [30]. However, further studies need to be conducted to support this phenomenon.

Presence of both D614G and P681R mutations significantly enhanced the virus infectivity and cell-to-cell fusion

We examined the synthetic P681H, D614G+P681R and natural D614G, Alpha, Delta and Omicron variants pseudoviruses of their infectivity by measuring relative luciferase units in 293T overexpressing hACE2 and TMPRSS2 cells. As shown in Fig2a, the highest infectivity titers were found in D614G+P681R and Delta followed by D614G>Alpha>Omicron>P681H in 293T-hACE2 cell line. Additionally, all the variants also showed higher infectivity in 293T-TMPRSS2 overexpressed cell line as compared to wildtype pseudovirus, though the highest infectivity was shown in D614G+P681R >Delta>D614G variants (Fig2b). Omicron pseudoviruses showed ~2.18-1.52-fold rise in infectivity titer in hACE2 and TMPRSS2 respectively as compared to ancestral Wuhan-1 pseudoviruses (Fig2a-b). These data suggest as compared to Delta variant; Omicron, P681H and Alpha variants less efficiently use the TMPRSS2 receptor for virus entry. This is corroborated by the study of Meng Bo. et.al and group who have shown as

compared to Delta variant, the usage of TMPRSS2 receptor was lower in Omicron variant [31]. We further investigated fusion and syncytial formation by co-expressing spike variants either with hACE2 or TMPRSS2 or spike+hACE2+TMPRSS2 in BHK-21 cell line. Similar to earlier results, the highest fusion and syncytial formation was found in Delta and D614G+P681R mutants (Fig2c) when spike is co expressed with hACE2 plasmid. Furthermore, when spike variants were co expressed with TMPRSS2 alone, there was no fusion or syncytial formation (Fig 2d). However, when spike variants were co expressed along with hACE2 and TMPRSS2 together, the fusion and syncytial formation was markedly enhanced and highest being shown in Delta and D614G+P681R mutants (Fig2e-f). These data suggest the SARS-CoV-2 variants could efficiently carry out cell to cell fusion and syncytia in the cell lines where both hACE2 and TMPRSS2 receptors are well expressed. Meng Bo et.al and group have shown both ACE2 and TMPRSS2 receptors are well expressed in lungs and lower airway epithelial [31]. These data altogether might further explain why Delta variant could grow in high titer in lower respiratory lung cells where both ACE2 and TMPRSS2 are well expressed thus producing systemic infection, whereas Omicron has restricted growth mainly in upper respiratory epithelial cells where ACE2 is mainly expressed, thus producing local infection. Taken together, our data suggests D614G+P681H mutations found in Alpha and Omicron variants restricts the virus receptor usage mainly to ACE2 and lesser extent to TMPRSS2; whereas P681R along with D614G mutations allow the usage of both ACE2 and TMPRSS2 receptors, thus enhancing cell-to-cell fusion and infectivity and hence increase pathogenicity as shown in Delta variant.

P681R mutation (Delta variant) upregulates exogenous trypsin mediated fusion as compared to P681H mutation (Omicron variant)

As compared to ancestral wildtype virus, the variants and synthetic mutants pseudoviruses showed enhance virus entry mediated through hACE2 and TMPRSS2 receptor. The highest virus entry was shown in Delta variant and synthetic D614G+P681R mutant with >3-fold increase in virus entry in 293T overexpressing hACE2 and TMPRSS2 cells (Fig3a). In Omicron, Alpha and P681H mutants, virus entry was markedly higher in hACE2 cell line than TMPRSS2. The presence of proline in SARS-CoV-2 S1/S2 cleavage site “SPRRAR-SVAS” was found to be conserved not only in MERS-CoV and HCoV-NL63, but also in Influenza cleavage site sequence (Fig3b). Ord Mihkel et al and group have hypothesized, in the ancestral wildtype spike protein the presence of serine followed by proline in the cleavage site allows proline-directed phosphorylation which could modulate furin directed cleavage in ER-golgi pathway and fusion capacity [32]. We further sought to assess the effect of Proline to Arginine or Histidine mutation in spike variants’ in fusion and syncytia formation in the presence of exogenous trypsin. As shown in Fig3c in presence of exogenous trypsin there was significant increase in fusion and syncytial formation in D614G+P681R and Delta variant; however, there was no substantial increase in fusion in Alpha, Omicron or P681H spike variant, thus suggesting P681H mutation is not favorable for cell-to-cell fusion in presence of exogenous trypsin. However, presence of additional basic residue R in Delta variant “SRRRAR-SVAS” might be allowing more fusion in presence of trypsin like proteases. As shown in Fig3d., addition of trypsin enhanced the cleavability of Delta variant as compared to Alpha and Omicron variant.

VoC pseudoviruses including Omicron pseudovirus' entry to host cell and fusion is significantly reduced in presence of Cathepsin L inhibitor

It has been previously reported that SARS-CoV-2 in presence of ACE2 receptor could rapidly endocytosed and could be cleaved by Cathepsin L proteases in the endosomal compartment, exposing the fusion peptide and initiating fusion process [33] (Fig.4a). We assessed the entry of pseudovirus variants when treated with Cathepsin L inhibitor E64d in the absence of TMPRSS2 [34,35]. As shown in Fig4b and 4c, in the absence of TMPRSS2, there was significant inhibition of virus entry in all the variants and synthetic mutants when treated with 20 μM of E64d as compared to ancestral wildtype pseudovirus. The highest inhibition of entry was shown in Delta, D614G and D614G+P681R variants. Omicron, Alpha and P681H spike mutants showed >50% inhibition of virus entry in presence of E64d. Additionally, in all the variants except wildtype and to lesser extent in Delta variant, the fusion was significantly reduced in presence of E64d (Fig.4d). Next, we evaluated the fusion of variants' spike protein when cells were treated with lysosomotropic agent ammonium chloride. Ammonium chloride helps in endosomal acidification which in turn modulates Cathepsin L mediated proteolytic activity [35]. In presence of 20mM NH_4Cl, the reduction in fusion was seen in all the variants and ancestral wildtype virus, where as in single P681H mutant to lesser extent. These results suggest, in absence of TMPRSS2, the Omicron could efficiently enter the cells via ACE2-dependent endocytosis and highly susceptible to Cathepsin L inhibitor like E64d.

Effect of TMPRSS2 inhibitor on pseudovirus variants entry and fusion

We further evaluated the effect of Camostat mesylate, which is TMPRSS2 serine protease inhibitor, on pseudo virus variants' entry and fusion. The D614G, Delta and D614G+P681R pseudovirus variants showed more than >60% reduction in virus entry to cells co expressing ACE2 and TMPRSS2 in presence of 100μM Camostat mesylate (Fig.5a). Whereas Omicron, P681H and Alpha variant pseudoviruses showed less than < 50% reduction in virus entry in presence of Camostat mesylate. This was in consistent with the earlier results that showed variants like Omicron or Alpha consisting of P681H mutation, majorly use ACE2 receptor for virus entry. In BHK-21 cells, the spike proteins of different variants were co expressed either in presence of TMPRSS2 alone or with ACE2 and TMPRSS2 together. Upon addition of Camostat mesylate, the fusion or syncytial formation was found to be diminished in all variants (Fig5b and 5c). However, as compared to E64d, the effect of Camostat mesylate was low in inhibiting fusion in variants.

Omicron pseudoviruses stability, S1 shedding and cross reactivity to recombinant soluble Delta RBD polyclonal sera

The SARS-CoV-2 pseudoviruses loss their titer as measured by relative luciferase units (RLU) when subjected to repeated freeze thaw or stored at -80°C for longer period, which might be due to shedding of S1 domain. Zhang L et.al and group have showed D614G mutation allowed decrease in S1 shedding thus presence of more functional whole spike virion which enhances infectivity [36]. Hence, we sought to test the stability of Omicron spike incorporated into the HIV-1 backbone by repeated freeze-thaw of

pseudovirus particles and then measuring the infectivity titer as expressed in relative luciferase units (RLU). As compared the Delta and D614G variant, the Omicron pseudovirions infectivity titer was impaired when subjected to two times freeze-thaw (Fig.6a). We further assessed the S1 shedding of Omicron pseudoviruses when kept at room temperature and in presence of soluble hACE2. As shown in Western blot analysis Fig.6b, in the ancestral spike protein the S1 shedding was more pronounced, whereas no S2 band was seen in Alpha and Omicron pseudoviruses supernatant. A faint band of S2 was seen in Delta pseudovirus supernatant. Overall, the data suggests, variants spike proteins were more stable than ancestral spike protein. Omicron spike protein contains ~33 mutations which might have changed the spike conformation and antigenicity, for which there was observance of reduced neutralization efficacy against major vaccines [28]. We further test the ability of polyclonal sera raised in mouse against recombinant soluble RBD Delta protein to recognize the Omicron spike protein when expressed in BHK-21 cell line. The BHK-21 cells were transfected with ancestral wildtype, Alpha, Delta and Omicron spike and 36 h post transfection, were probed with mouse polyclonal sera raised against soluble ancestral RBD and Delta RBD (L452R and T478K mutations). As shown in Fig.6c, Alpha, Delta and Omicron spikes were well recognized by ancestral RBD sera and Delta RBD sera. Future experiments are planned to assess the cross neutralization of immunized sera with different soluble RBD proteins against different VoC viruses, which could provide greater clarity on effect of antigenicity and immunogenicity.

Additionally, as compared to the ancestral wild type virus alpha and Delta live viruses grow slowly and produce small plaques and produce less virus titer in Vero E6 cells which are routinely used for in vitro studies (Supplementary Fig.3). In contrast, Omicron live virus does not produce cytopathic effect in Vero E6 and for in vitro studies, Omicron live viruses are grown in Calu-3 cells [37]. Vero E6 cells are deficient in ACE2 and TMPRSS2 receptors, which might be the reason of slow growth of variants and less CPE in Vero E6 cell line as compared to ancestral virus which could non-specifically enter the Vero E6 cells [38].

Taken altogether, our results elucidate the interplay between the evolution of SARS-CoV-2 virus with introduction of D614G and cleavage site mutations which might be impacting virus entry and thus modulating virus transmission, pathogenesis and disease severity (Fig.6d).

Discussion

Virus entry and fusion are two important phenomena that determines the disease severity, transmission and infectivity. With the emergence of novel SARS-CoV-2 and its variants of concern, new pandemic wave continues to impact enormous economic loss and crippling the health care system all over the world. The current available vaccines are targeted to spike domain which is the most immunogenic region. The introduction of new mutations in the SARS-CoV-2 virus is mainly in the spike domain, which is resulting in immune escape and drastic reduction in neutralization efficacy to current vaccines [37,39–41]. Hence, it is utmost important to understand the virus entry and fusion mechanism of emerging variants. SARS-CoV-2 is an enveloped RNA virus and studies from important other RNA viruses such as Influenza, HIV-1 have shown that RNA viruses selectively introduce mutation for virus transmission, infectivity and fitness[42]

and mutants with deleterious fitness mutations slowly disappear. Tracking the major SARS-CoV-2 variants of concerns have shown the presence of D614G and cleavage site P681R/H mutations in spike protein, which might be an indicator of infectivity and disease transmission (Fig1a).

The introduction of mutations in the spike region changes the conformation as shown previously with D614G, Alpha and Delta variants, thus modulating the binding to hACE2 receptor which in turns determine virus entry and immune escape to vaccines [43–45] Here, we have shown that variants including Omicron spike and synthetic spike mutants expressed on surface binds to soluble-hACE2 at a higher fold as compared to ancestral spike protein (Fig1b), which corroborates with other reported studies [46,47]. Furthermore, we have found that all the variants, including Omicron pseudoviruses showed significant increase in infectivity titer in 293T-hACE2 cells (Fig2a); however as compared to Delta variant, the infectivity titer did not increase in TMPRSS2 expressed 293T cell line. Delta variant have shown to use both ACE2 and TMPRSS2 protease mediated virus entry [48]. The synthetic double mutant D614G+P681R has also showed high infectivity titer in both ACE2 and TMPRSS2 overexpressed cells, thus indicating the potential role of these two mutations in ACE2 and TMPRSS2 mediated virus entry. In addition, assessment of fusion and syncytial formation of these spike variants and synthetic mutants further showed that presence of D614G and P681R mutation significantly enhanced the fusogenic property and syncytial formation (Fig2b-e). Interestingly, even the Omicron spike harbors ~33 mutations, there is marked reduction in fusion capacity of Omicron pseudoviruses. Presence of P681H mutation might be attributing to low fusogenic property of Omicron spike protein. However, the role of other mutations in Omicron spike might have an impact on virus biology. Nevertheless, the Delta variant has shown to enhance virus entry in both hACE2 and TMPRSS2 over expressed cells, whereas Omicron pseudoviruses showed preference to hACE2-mediated virus entry (Fig3a).

Presence of multi-basic cleavage site sequence in viral envelopes allow efficient cleavage by furin like proteases [49] and determines virus pathogenesis and virulence [50]. Further assessment of SARS-CoV-2 variants spike proteins has shown P681R mutation allows increase cell-to-cell fusion in presence of exogenous trypsin as shown in Delta and double D614G+P681R mutant spike but not with Omicron spike which has P681H mutation and single P681H mutant (Fig 3c). This data suggests presence of P681H mutation in Omicron spike cleavage site down regulates cleavability of spike protein by furin or trypsin like proteases, thus restricting localized replication of Omicron virus.

Peacock. P.T et, al and group have recently shown [29], Omicron viruses usage TMPRSS2 independent entry pathway. In our study, we found both the variants and mutants pseudoviruses entry to host cell is markedly reduced when treated with Cathepsin L inhibitor like E64d (Fig.4). In the P681H mutant, introduction of single mutation near cleavage site has greatly modulated the virus entry and fusion in presence of E64d or NH4Cl. Our study showed Omicron pseudoviruses titer increased in ACE2 cell line and virus entry could reduce to more than 50% in presence of E64d, where as in presence of TMPRSS2 inhibitor Camostat mesylate, there was only ~34% reduction in virus entry (Fig.5a). These findings suggests Omicron spike preferentially enter through ACE2-mediated endocytosis and this is in support

with recent studies which showed Omicron preferentially enters cells by endocytic pathway [29,51]. In contrast, highly virulent variants like Delta could use both a) endocytic pathway and activation of S1/S2 protein mediated by Cathepsin B/L proteases and b) cell surface entry by activation of S1/S2 using serine protease TMPRSS2. Previous studies on SARS-CoV have reported entry of viruses into lungs mainly mediated by TMPRSS2 which is highly expressed in lower respiratory tract [52]. Presence of P681R in Delta cleavage site, adds another basic residue in cleavage site and Serine amino acid which is present near the cleavage site, might be more accessible by serine proteases as compared to Omicron spike cleavage site in which P-681 was replaced by Histidine. Moreover, the serine and other proteases requires the accessibility to furin recognition motif and extended loop length for proper proteolytic cleavage [53]. Mutation of P681 to R might be allowing better accessibility of both intra and extra cellular proteases to act on spike cleavage site. However, more studies are needed to temper this observation.

Additionally, the ancestral SARS-CoV-2 viruses have shown to enter and replicate in Vero-E6 cell line in vitro (which are deficient in ACE2 and TMPRSS2 receptor) by non-specific endocytic uptake and further cleavage processing in late endosomal-lysosome compartments [54–56]. Whereas, the variants like Alpha, Delta grow slow and produce small plaques in Vero E6 (Supplementary Fig.3) and Omicron does not produce CPE or grow in Vero E6, suggesting variants requires ACE2 or TMPRSS2 dependent activation of S1/S2 protein or both for entry to host cells.

In our findings, the variants spike proteins showed marked rise in surface expression in 293T cells as compared to ancestral virus (Supplementary fig.2), further suggesting the D614G and P681H/R mutations could efficiently support spike processing and transport through ER-Golgi pathway to surface. Spike density in virus and stability of spike protein is also a major determinant of virus virulence and immune escape. D614G mutation have shown to be more stable and in presence of hACE2, the S1 shedding has been found to be reduced [57,58]. Our study is in corroboration with the earlier findings and we found even after repeated freeze-thaw the variants are more stable than the ancestral virus (Fig.6). Additionally, the soluble-hACE2 induced shedding of S1 domain is lower in variants as compared to wildtype spike protein (Fig.6b)

In summary, we show that that presence of D614G and P681R mutations are crucial for SARS-CoV-2 variants virulence and pathogenesis as seen with Delta variant. In the Omicron virus though there is presence D614G mutation, but P681H mutation might have resulted in slow processing of cleavage by furin or trypsin like proteases and allows ACE2-dependent entry thus restricting the Omicron virus replication mainly to upper respiratory tract. Although we have not studied the role of other mutations present in Omicron spike protein, the single synthetic mutant P681H phenotypically behaving more similar to that of Omicron. Understanding the virus entry pathway, will further allow us in appropriate selection of cell lines for in vitro screening of drugs and vaccine candidates and development of novel drugs. The variants of concerns like Delta and Omicron demonstrated evolution of both virulent and moderately virulent strains, for better fitness for survival.

Methods

Plasmids, viruses and cell lines

The full-length spike of the SARS-CoV-2 isolate Wuhan-Hu-1, (GenBank: MN908947.3, Surface glycoprotein) was codon optimized, cloned in pcDNA3.1 vector and gene synthesized by Thermo Fisher Scientific, Invitrogen USA. HIV-1 pNL4-3.Luc.R-E- plasmid NIH AIDS reagent, a kind gift from Dr.Kalpana Luthra, AIIMS, India. Delta recombinant RBD for soluble RBD preparation was prepared by site directed mutagenesis and introducing L452R+T478K mutation in backbone of the Wu-1 strain of RBD from BEI (Catalog No. NR-52422; BEI Resources; NIH). TMPRSS2 plasmid was obtained from Addgene (Catalogue no. 53887. pCAGGS- SARS CoV 2 soluble stabilized spike, with His tag, NR-52394 was obtained from BEI Resources. SARS-CoV-2, hCoV-19/USA/PHC658/2021 (B.1.617.2) live virus (NR-55611), SARS-CoV-2, hCoV-19/USA/CA-SU-15_S02/2021 b.1.617 (Vero/T) (NR-55486), SARS-CoV-2, hCov-19/England/204820464/2020 (NR-54000), SARS-Related Coronavirus 2, Isolate USA-WA1/2020 (NR-52281), HEK 293T over expressing ACE2 cell line (NR52511) were obtained from BEI Resources, USA. Vero E6 and BHK-21 cell lines are kind gift from Dr.Sudhanshu Vrati, RCB, India. ACE2-Fc plasmid is kind gift Prof. S Pöhlmann, Infection Biology Unit, Göttingen, Germany. HEK293T, HEK293T-hACE2, Vero E6 cells, BHK-21 cells were cultured in DMEM with 10% fetal bovine serum (FBS), 1% glutamax and 1% penicillin/streptomycin and routinely tested for mycoplasma free.

Pseudo virus production, infectivity titer and virus entry assay

293T cells were seeded in 6 well plate at density of 0.4×106 cells/ well, after 24 hr of incubation cells were fed with fresh medium. Pseudoviruses were prepared as described previously[59] with few modifications. Briefly, 293T cells were transiently transfected with Spike plasmid and backbone pNL4-3.Luc.R-E- using HD Promega Fugene in OptiMEM media and maintained in DMEM growth media at 37°C and 5% CO2. After 48 h of incubation the supernatants containing virions pseudotyped with SARS-CoV-2S were harvested and clarified with centrifugation, aliquoted and stored at -80°C. Each supernatant was used once and fresh pseudoviruses were prepared every 10 days. The pseudoviruses were titered in 293T-hACE2 cell line. For infection titer, 293T over expressed hACE2 cells, BEI Resources NR52511 (40000 cells/well in 96 well plate) were seeded into 100µl of pseudovirus supernatant and 48-hour post infection cells were lysed with britelite plus reporter substrate (Perkin Elmer) and luminescence was measured by PerkinElmer luminometer. For TMPRSS2 expression, 293T cells were transfected with 10µg of TMPRSS2 plasmid using HD Fugene transfecting reagent. 24h post transfection, cells are harvested and used for measuring pseudovirus infectivity titer. For virus entry study, 40000 cells/well were seeded into 96-well plates and after 4 hours, equal viral supernatant that gave ~75,000 relative luciferase units were chosen for infection for virus entry assay.

Soluble hACE2 and Delta RBD production and purification

Soluble hACE2, soluble Delta RBD, soluble pre-fusion spike proteins were expressed in transiently transfected Expi293F cells in suspension culture using Expi293fectin (Invitrogen) following manufactures

protocol. Cell culture supernatants were harvested 5–6 days after transfection. For protein purification, the supernatant was passed through a Ni-NTA column for His tagged protein and protein A affinity column for Fc tagged protein. Bound proteins were eluted either with 500 mM Imidazole (His tagged protein) and 100Mm glycine, pH 2.5 (Fc tagged protein) and further purified by SEC using Superdex 200 (10/30) column (GE Biosciences). Eluted proteins were concentrated with an Amicon filter (Millipore; 10 kDa) and protein fractions were aliquoted and stored at −80 °C until further use.

Western blot

The SARS-CoV-2 spike glycoprotein was detected in cells by using western blot. Briefly, HEK293T cells were co-transfected with the S and HIV-1 pNL4-3.Luc.R-E- plasmid backbone as discussed above. After 24 and 48 hours of transfection, supernatant was harvested, pseudovirus were pellet down by using 20% sucrose cushion using ultracentrifuge at 25,000 rpm for 2 h at 4 °C and virus pellets were lysed with 30 µl RIPA buffer (20mM Tris-HCl pH 7.5, 150mM NaCl, 1mM EDTA, 0.1% SDS, 1% NP40, 1×protease inhibitor cocktail). After sonication at the amplitude of 10 for 2 mins, cell lysates were heated for 10 minutes at 100°C, centrifuged and separated in a 10% sodium dodecyl sulphate-polyacrylamide (SDS-PAGE) gel and transferred to a polyvinylidene fluoride (PVDF) membrane. The membrane was blocked with 5% skimmed milk, incubated with anti-spike mouse polyclonal sera (1:500) for overnight at 4°C. The membrane was developed with HRP-conjugated anti-mouse secondary antibody (1:2000, Jackson ImmunoResearch, PA, USA).

For the trypsin-based spike cleavage analysis, the spike transfected cells were treated with TPCK-trypsin (2mg/ml) for one hour in DMEM only after 24 hour of transfection and later incubated with 10% FBS containing DMEM for one hour. After this treatment, cell lysate preparation and western blotting were performed in the above-mentioned way.

FACS-based surface expression and soluble hACE2 binding assay

FACS-based cell surface expression assay was carried out as described previously[60]. Briefly, 293T cells were transiently transfected with different variant spike plasmids using HD Fugene transfecting reagent (Promega,USA). 24 h post transfection, cells were harvested with 5mM EDTA, washed three times with FACS buffer (DMEM + 5% HIFBS) and incubated with anti-spike mouse polyclonal sera for 1h at room temperature (RT). Anti-spike sera were raised in mouse by immunizing 20 µg of SARS CoV 2 soluble stabilized spike-His tag (NR-52394, BEI Resources) protein along with AddaVax by 0 day prime, 28-day boost and sera were collected after 14 days boost and used in all assays (Western blot, Immunofluroscence, FACS). The cells were washed three times with FACS buffer and then stained with PE-conjugated goat anti-mouse secondary antibody (1:200 dilutions, Jackson ImmunoResearch) for 1 h at RT. The cells were again washed three times with FACS buffer and fixed with 0.5% paraformaldehyde. The stained cells were then analyzed in a FACS Canto analyzer (BD Biosciences) and data analyzed with FlowJo software (version 10.0.6, Tree Star Inc). The data were expressed as mean fluorescent intensity (MFI).

For hACE2-spike binding assay, HEK-293T cells were transfected with either ancestral or variants spike plasmids and 24h post transfection, cells were harvested with 5 mM EDTA, washed twice with 5% FBS in 1×PBS, and then incubated with 4 µg/ml soluble hACE2 for 1 h in ice. After the incubation cells were washed three times with FACS buffer, and incubated with polyclonal goat anti human ACE2 antibody (1:200) (R&D Systems,USA) for 1 h, followed by 1h incubation with PE-conjugate goat-anti human secondary antibody (1:1000) (Jackson ImmunoResearch, USA). After washing, cells were then analyzed with FlowJo software (version 10.0.6, Tree Star Inc). The data were expressed as mean fluorescent intensity (MFI).

Qualitative fusion and syncytial formation assay

0.1 million BHK-21 cells were seeded in each well of a 24-well plate and the plate was incubated at 37°C with 5% CO_2. After 24 hours, cells were transfected with 0.5 µg of Spike and/or ACE2 and/or TMPRSS2 expressing plasmids using HD FuGENE transfecting reagent at the1:3 DNA:FuGENE ration (Promega, E2311) using Opti-MEM media. After 30 minutes of incubation at room temperature, this mixture was added to the cells and the plate was incubated at 37°C with 5% CO_2. For fusion inhibition assay after 2 hours, inhibitors like E-64d (20uM, Sigma-Aldrich, E8640), Camostat Mesylate (100Um, Sigma-Aldrich, SML0057) and ammonium chloride (20mM, Sigma-Aldrich, 254134) were added to the respective wells. For tryspin dependent cell-cell fusion, after 22 hours of transfection, one-hour TPCK-trypsin (2mg/ml) treatment was given to the respective well in DMEM media without FBS. Later, the media was changed with complete DMEM having 10% FBS. Cells were fixed after 24 hours of transfection in 4% paraformaldehyde for 15 min, then penetrated with 0.1% triton in PBS for 10 min. Non-specific binding was blocked using 3% goat serum in PBS for 1 h at room temperature. Cells were then incubated for overnight at 4°C with the anti-Spike polyclonal sera (1:200). To check the cross reactivity, with Delta protein induced sera, anti-Delta RBD mouse polyclonal sera was used as primary antibody. Next day, cells were washed three times with PBS and incubated for 1 h at room temperature with Alexa488-labeled rabbit anti-mouse IgG (1:1000). Three washes were given and the cell nuclei were counterstained with DAPI (D9542, Sigma-Aldrich, United States) for another 10 min at room temperature. The expression of proteins was observed by fluorescence microscope (IX-71, Olympus).

Quantitative fusion assay

Forty thousand HEK-293T cells were seeded in a 96-well plate. After 24 hours, cells were co-transfected with plasmids encoding CoV-2 S glycoprotein and pNL4-3.Luc.R-E- plasmid backbone expressing luciferase. After 24 hours of transfection, ACE2 and ACE2 + TMPRSS2 over expressing HEK-293T cells were overlaid on spike transfected HEK293T cells. After 16 hours, cells were lysed with britelite plus reporter substrate (Perkin Elmer) and luminescence was measured by PerkinElmer luminometer.

Live virus plaque assay

SARS-CoV-2 ancestral and variants live virus growth as measured by plaque formation was performed in Vero E6 cells as described previously[61] in THSTI Infectious Disease Research Facility (Biosafety level 3

facility). Briefly, and 80%confluent Vero E6 cells in 12-well plates were infected with serially diluted viruses for 1 h at 37°C after removing the growth medium. After 1 h of adsorption, the plate was washed one time with Dulbecco's Modified Eagle Medium (DMEM) growth media and overlaid with DMEM growth medium containing 2% carboxy methylcellulose (CMC) and incubated at 37°C. Forty-eight hours p.i., the overlay was removed and the cells were washed with PBS and fixed in 6% formalin for inactivation of virus for 4 h at RT. The fixed-cell monolayers were stained with 1% crystal violet for 30 min at RT and washed under running tap water. The plates were allowed to air dry, and the plaques were visualized and counted by eye.

Virus entry inhibitor assay

Forty thousand HEK-293T cells were seeded in a 96-well plate. After 24 hours, cells were co-transfected with plasmids encoding CoV S glycoprotein and pNL4.3 backbone expressing luciferase as described above. After 24 hours of transfection, ACE2 and ACE2 + TMPRSS2 over expressing HE293T cells were overlaid on previous day transfected HEK293T cells. E64d (20uM) and Camostat mesylate (100uM) were also added to the respected wells along with the cells. After 16 hours, cells were lysed with britelite substrate and luminescence was measured by PerkinElmer luminometer.

Statistical analysis

All assays were performed repeated two times or more and data is plotted as the mean and the error bar indicates the ±SD. Results were analyzed on GraphPad Prism version 7 (GraphPad Software Inc.). Significant differences were calculated by comparing ancestral wild type with other variants using one-way Anova (analysis of variance) with Bonferroni’s multiple comparisons test. Values were considered statistically significant for the p values obtained below 0.05. P values are presented as asterisks as *P <0.05, **P<0.01, ***P<0.001, ****P<0.0001 considered significant.

Data availability

The data supporting the findings of this study are available from the corresponding author upon request. The source data underlying Figs. 1b-c, 2a-e, 3a,c,d, 4 b-d , 5a-c, and 6a, b and Supplementary Figs. 1, 2 and 3 are provided as a Source Data file.

References

1. Kahn, J. S. & McIntosh, K. History and recent advances in coronavirus discovery. *Pediatr. Infect. Dis. J.* **24**, (2005).

2. Borges, V. *et al.* Mutation rate of SARS-CoV-2 and emergence of mutators during experimental evolution. *bioRxiv* 2021.05.19.444774 (2021) doi:10.1101/2021.05.19.444774.

3. Bar-On, Y. M., Flamholz, A., Phillips, R. & Milo, R. SARS-CoV-2 (COVID-19) by the numbers. *Elife* **9**, (2020).

4. Abdelrahman, Z., Li, M. & Wang, X. Comparative Review of SARS-CoV-2, SARS-CoV, MERS-CoV, and Influenza A Respiratory Viruses. *Frontiers in Immunology* vol. 11 (2020).

5. Otto, S. P. *et al.* The origins and potential future of SARS-CoV-2 variants of concern in the evolving COVID-19 pandemic. *Curr. Biol.* **31**, R918 (2021).

6. Papanikolaou, V. *et al.* From Delta to Omicron: S1-RBD/S2 mutation/deletion equilibrium in SARS-CoV-2 defined variants. *Gene* **814**, 146134 (2022).

7. Zhang, X. *et al.* SARS-CoV-2 Omicron strain exhibits potent capabilities for immune evasion and viral entrance. *Signal Transduct. Target. Ther.* **6**, 10–12 (2021).

8. Plante, J. A. *et al.* Spike mutation D614G alters SARS-CoV-2 fitness. *Nature* **592**, 116–121 (2021).

9. Frampton, D. *et al.* Genomic characteristics and clinical effect of the emergent SARS-CoV-2 B.1.1.7 lineage in London, UK: a whole-genome sequencing and hospital-based cohort study. *Lancet. Infect. Dis.* **21**, 1246–1256 (2021).

10. Hou, Y. J. *et al.* SARS-CoV-2 D614G variant exhibits efficient replication ex vivo and transmission in vivo. *Science* **370**, 1464–1468 (2020).

11. Kraemer, M. U. G. *et al.* Spatiotemporal invasion dynamics of SARS-CoV-2 lineage B.1.1.7 emergence. *Science* **373**, 889–895 (2021).

12. Hoffmann, M., Kleine-Weber, H. & Pöhlmann, S. A Multibasic Cleavage Site in the Spike Protein of SARS-CoV-2 Is Essential for Infection of Human Lung Cells. *Mol. Cell* **78**, 779-784.e5 (2020).

13. Xie, X. *et al.* Neutralization of SARS-CoV-2 spike 69/70 deletion, E484K and N501Y variants by BNT162b2 vaccine-elicited sera. *Nat. Med.* **27**, 620–621 (2021).

14. Cherian, S. *et al.* SARS-CoV-2 Spike Mutations, L452R, T478K, E484Q and P681R, in the Second Wave of COVID-19 in Maharashtra, India. *Microorganisms* **9**, (2021).

15. Mlcochova, P. *et al.* SARS-CoV-2 B.1.617.2 Delta variant replication and immune evasion. *Nature* **599**, (2021).

16. Yang, W. & Shaman, J. COVID-19 pandemic dynamics in India, the SARS-CoV-2 Delta variant, and implications for vaccination. *medRxiv Prepr. Serv. Heal. Sci.* (2021) doi:10.1101/2021.06.21.21259268.

17. Thiruvengadam, R. *et al.* Effectiveness of ChAdOx1 nCoV-19 vaccine against SARS-CoV-2 infection during the delta (B.1.617.2) variant surge in India: a test-negative, case-control study and a mechanistic study of post-vaccination immune responses. *Lancet. Infect. Dis.* (2021) doi:10.1016/S1473-3099(21)00680-0.

18. Peacock, T. P. *et al.* The SARS-CoV-2 variant, Omicron, shows rapid replication in human primary nasal epithelial cultures and efficiently uses the endosomal route of entry. *bioRxiv Prepr. Serv. Biol.* (2022) doi:10.1101/2021.12.31.474653.

19. Baric, R. S. Emergence of a Highly Fit SARS-CoV-2 Variant. *N. Engl. J. Med.* **383**, 2684–2686 (2020).

20. Hoffmann, M. *et al.* SARS-CoV-2 Cell Entry Depends on ACE2 and TMPRSS2 and Is Blocked by a Clinically Proven Protease Inhibitor. *Cell* **181**, 271-280.e8 (2020).

21. Hwang, S. S. *et al.* Cryo-EM structure of the 2019-nCoV spike in the prefusion conformation. *Science* **367**, 1255–1260 (2020).

22. Lukassen, S. *et al.* SARS-CoV-2 receptor ACE2 and TMPRSS2 are primarily expressed in bronchial transient secretory cells. *EMBO J.* **39**, (2020).

23. Lamers, M. M. *et al.* SARS-CoV-2 productively infects human gut enterocytes. *Science* **369**, 50–54 (2020).

24. Chen, L., Li, X., Chen, M., Feng, Y. & Xiong, C. The ACE2 expression in human heart indicates new potential mechanism of heart injury among patients infected with SARS-CoV-2. *Cardiovasc. Res.* **116**, 1097–1100 (2020).

25. Jing, Y. *et al.* Potential influence of COVID-19/ACE2 on the female reproductive system. *Mol. Hum. Reprod.* **26**, 367–373 (2020).

26. Yang, N. & Shen, H. M. Targeting the Endocytic Pathway and Autophagy Process as a Novel Therapeutic Strategy in COVID-19. *Int. J. Biol. Sci.* **16**, 1724–1731 (2020).

27. Tang, T., Bidon, M., Jaimes, J. A., Whittaker, G. R. & Daniel, S. Coronavirus membrane fusion mechanism offers a potential target for antiviral development. *Antiviral Res.* **178**, (2020).

28. Wilhelm, A. *et al.* Reduced Neutralization of SARS-CoV-2 Omicron Variant by Vaccine Sera and Monoclonal Antibodies. *medRxiv* 2021.12.07.21267432 (2021) doi:10.1101/2021.12.07.21267432.

29. Peacock, T. P. *et al.* The SARS-CoV-2 variant, Omicron, shows rapid replication in human primary nasal epithelial cultures and efficiently uses the endosomal route of entry. *bioRxiv* 2021.12.31.474653 (2022) doi:10.1101/2021.12.31.474653.

30. Ueo, A. *et al.* Lysosome-Associated Membrane Proteins Support the Furin-Mediated Processing of the Mumps Virus Fusion Protein. *J. Virol.* **94**, (2020).

31. Bo Meng, Steven A Kemp, Guido Papa, Rawlings Datir, Isabella A T M Ferreira, Sara Marelli, William T Harvey, Spyros Lytras, Ahmed Mohamed, Giulia Gallo, Nazia Thakur, Dami A Collier, Petra Mlcochova,

COVID-19 Genomics UK (COG-UK) Consortium; Lidia M Dunca, R. K. G. Recurrent emergence of SARS-CoV-2 spike deletion H69/V70 and its role in the Alpha variant B.1.1.7. *Cell Rep.* **35**, (2021).

32. Örd, M., Faustova, I. & Loog, M. The sequence at Spike S1/S2 site enables cleavage by furin and phospho-regulation in SARS-CoV2 but not in SARS-CoV1 or MERS-CoV. *Sci. Rep.* **10**, (2020).

33. Plante, J. A. *et al.* Spike mutation D614G alters SARS-CoV-2 fitness. *Nat. 2020 5927852* **592**, 116–121 (2020).

34. Ou, X. *et al.* Characterization of spike glycoprotein of SARS-CoV-2 on virus entry and its immune cross-reactivity with SARS-CoV. *Nat. Commun.* **11**, (2020).

35. Ou, T. *et al.* Hydroxychloroquine-mediated inhibition of SARS-CoV-2 entry is attenuated by TMPRSS2. *PLoS Pathog.* **17**, (2021).

36. Zhang, L. *et al.* SARS-CoV-2 spike-protein D614G mutation increases virion spike density and infectivity. *Nat. Commun.* **11**, (2020).

37. Medigeshi, G. *et al.* Sub-optimal Neutralisation of Omicron (B.1.1.529) Variant by Antibodies induced by Vaccine alone or SARS-CoV-2 Infection plus Vaccine (Hybrid Immunity) post 6-months. *medRxiv* 2022.01.04.22268747 (2022) doi:10.1101/2022.01.04.22268747.

38. Murgolo, N. *et al.* SARS-CoV-2 tropism, entry, replication, and propagation: Considerations for drug discovery and development. *PLoS Pathog.* **17**, (2021).

39. Planas, D. *et al.* Reduced sensitivity of SARS-CoV-2 variant Delta to antibody neutralization. *Nature* **596**, 276–280 (2021).

40. Davis, C. *et al.* Reduced neutralisation of the Delta (B.1.617.2) SARS-CoV-2 variant of concern following vaccination. *PLoS Pathog.* **17**, e1010022 (2021).

41. Lazarevic, I., Pravica, V., Miljanovic, D. & Cupic, M. Immune Evasion of SARS-CoV-2 Emerging Variants: What Have We Learnt So Far? *Viruses* **13**, (2021).

42. Dolan, P. T., Whitfield, Z. J. & Andino, R. Mapping the Evolutionary Potential of RNA Viruses. *Cell Host Microbe* **23**, 435–446 (2018).

43. Weisblum, Y. *et al.* Escape from neutralizing antibodies by SARS-CoV-2 spike protein variants. *Elife* **9**, 1 (2020).

44. Harvey, W. T. *et al.* SARS-CoV-2 variants, spike mutations and immune escape. *Nat. Rev. Microbiol.* **19**, 409–424 (2021).

45. Ahmad, L. Implication of SARS-CoV-2 Immune Escape Spike Variants on Secondary and Vaccine Breakthrough Infections. *Front. Immunol.* **12**, (2021).

46. Yin, W. *et al.* Structures of the Omicron spike trimer with ACE2 and an anti-Omicron antibody: mechanisms for the high infectivity, immune evasion and antibody drug discovery. *bioRxiv* 2021.12.27.474273 (2021) doi:10.1101/2021.12.27.474273.

47. Ni, D. *et al.* Structural analysis of the Spike of the Omicron SARS-COV-2 variant by cryo-EM and implications for immune evasion. *bioRxiv* 2021.12.27.474250 (2021) doi:10.1101/2021.12.27.474250.

48. Mlcochova, P. *et al.* SARS-CoV-2 B.1.617.2 Delta variant replication and immune evasion. *Nature* **599**, (2021).

49. Peacock, T. P. *et al.* The furin cleavage site in the SARS-CoV-2 spike protein is required for transmission in ferrets. *Nat. Microbiol.* **6**, 899–909 (2021).

50. Schrauwen, E. J. A. *et al.* Insertion of a multibasic cleavage site in the haemagglutinin of human influenza H3N2 virus does not increase pathogenicity in ferrets. *J. Gen. Virol.* **92**, 1410–1415 (2011).

51. Willett, B. J. *et al.* The hyper-transmissible SARS-CoV-2 Omicron variant exhibits significant antigenic change, vaccine escape and a switch in cell entry mechanism. *medRxiv* 2022.01.03.21268111 (2022) doi:10.1101/2022.01.03.21268111.

52. Shyr, Z. A., Gorshkov, K., Chen, C. Z. & Zheng, W. Drug Discovery Strategies for SARS-CoV-2. *J. Pharmacol. Exp. Ther.* **375**, 127–138 (2020).

53. Laporte, M. *et al.* The SARS-CoV-2 and other human coronavirus spike proteins are fine-tuned towards temperature and proteases of the human airways. *PLoS Pathog.* **17**, (2021).

54. Mercer, J. & Helenius, A. Virus entry by macropinocytosis. *Nat. Cell Biol.* **11**, 510–520 (2009).

55. Aleksandrowicz, P. *et al.* Ebola virus enters host cells by macropinocytosis and clathrin-mediated endocytosis. *J. Infect. Dis.* **204**, (2011).

56. Murgolo, N. *et al.* SARS-CoV-2 tropism, entry, replication, and propagation: Considerations for drug discovery and development. *PLoS Pathog.* **17**, (2021).

57. Zhang, L. *et al.* The D614G mutation in the SARS-CoV-2 spike protein reduces S1 shedding and increases infectivity. *bioRxiv Prepr. Serv. Biol.* (2020) doi:10.1101/2020.06.12.148726.

58. Plante, J. A. *et al.* Author Correction: Spike mutation D614G alters SARS-CoV-2 fitness. *Nature* **595**, E1 (2021).

59. Adedeji, A. O. *et al.* Novel inhibitors of severe acute respiratory syndrome coronavirus entry that act by three distinct mechanisms. *J. Virol.* **87**, 8017–8028 (2013).

60. Samal, S. *et al.* Cell surface ectodomain integrity of a subset of functional HIV-1 envelopes is dependent on a conserved hydrophilic domain containing region in their C-terminal tail. *Retrovirology* **15**,

(2018).

61. Vishwakarma, P. *et al.* Severe Acute Respiratory Syndrome Coronavirus 2 Spike Protein Based Novel Epitopes Induce Potent Immune Responses in vivo and Inhibit Viral Replication in vitro. *Front. Immunol.* **12**, (2021).

Declarations

Acknowledgements

We sincerely thank Prof Pramod Kumar Garg, Executive Director, THSTI for full support and valuable inputs and guidance. We thank Prof. S Pöhlmann, Infection Biology Unit, Göttingen, Germany for providing ACE2-Fc plasmids as a kind gift. We thank Dr. B Graham (VRC/NIAID/NIH) for providing us the spike construct (SARS-2-CoV S 2P). The following reagent was deposited by the Centers for Disease Control and Prevention and obtained through BEI Resources, NIAID, NIH: SARS Related Coronavirus 2, Isolate USA-WA1/2020, NR-52281. The following reagent was obtained through BEI Resources, NIAID, NIH: SARS-Related Coronavirus 2, Isolate hCoV-19/USA/PHC658/2021 (Lineage B.1.617.2; Delta Variant), NR-55611, contributed by Dr. Richard Webby and Dr. Anami Patel. The following reagent was obtained through BEI Resources, NIAID, NIH: SARS-Related Coronavirus 2, Isolate hCoV-19/USA/CA-Stanford-15_S02/2021 (Lineage B.1.617.1; Kappa Variant), NR-55486, contributed by Dr. Mehul Suthar and Dr. Benjamin Pinsky. The following reagent was obtained through BEI Resources, NIAID, NIH: SARS-Related Coronavirus 2, Isolate hCoV-19/England/204820464/2020, NR-54000, contributed by Bassam Hallis. The following reagent was obtained through BEI Resources, NIAID, NIH: Human Embryonic Kidney Cells (HEK-293T) Expressing Human Angiotensin-Converting Enzyme 2, HEK-293T-hACE2 Cell Line, NR-52511. TMPRSS2 plasmid was a gift from Roger Reeves (Addgene plasmid # 53887).The following reagent was contributed by David Veesler for distribution through BEI Resources, NIAID, NIH: Vector pcDNA3.1(-) Containing the SARS-Related Coronavirus 2, Wuhan-Hu-1 Spike Glycoprotein Receptor Binding Domain (RBD).We thank Dr. Ramandeep Singh for supporting on live virus work inside BSL3 in the Translational Health Science and Technology Institute (THSTI), Infectious Disease Research Facility (IDRF facility).We would like to thank THSTI FACS and Confocal core facility for the flow cytometry and immunofluorescence work. The sequencing of mutants was carried out at the Advanced Technology Platform Centre (ATPC) of Regional Centre for Biotechnology (RCB), and is funded by the Department of Biotechnology, Govt. of India (Grant No. BT.MED-II/ATPC/BSC/01/2010). We would like to thank Mr. Aman Gupta for coordinating the timely purchase of reagents. We would like to thank Mr. Satish Kumar and Mr. Deepak Badoni for coordinating with BEI Resources for SARS-CoV-2 related viruses and reagents.

Author contributions

S.S. and R.K conceived the project. S.S, A.A, S.A. coordinated the projects. R.K.,G.S, conducted majority of the experiments with the help of P.V, V.K., B.L, A.G. Sr.S, S.A; S.S, S.A,R.K, G.S, Sr.S and A.A analyzed the data. S.S wrote the original manuscript; A.A, S.A, R.K and P.V edited the manuscript.

Competing interests

The authors declare no competing interests.

Funding

This work was supported by the Department of Biotechnology (DBT), Govt. of India through THSTI core grant and GIISER-South Asia grant from Bill and Melinda Gates Foundation, Seattle, USA,

Figures

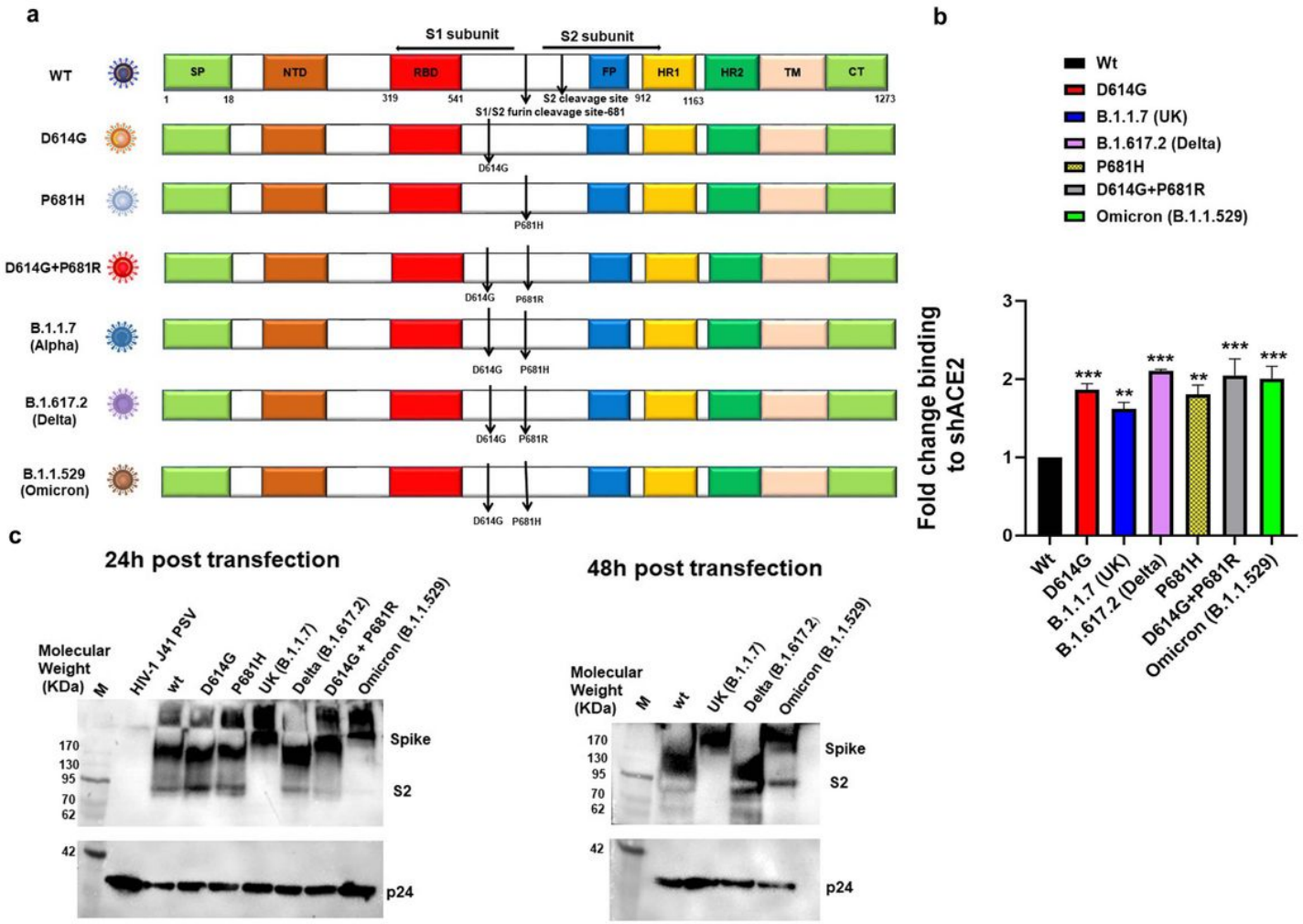

Figure 1

Expression and cleavage of SARS-CoV-2 variants and synthetic mutants: a. Schematic representation of ancestral, Alpha, Delta and Omicron spike protein with D614G and P681R/H mutations and synthetic mutants, the signal peptide (green box), S1-N terminal domain NTD (brown box), Receptor binding domain (Red box), fusion peptide (blue box),Heptad repeat 1(yellow box), Heptad repeat 2(dark green box), Transmembrane domain TM (Cream box), Cytoplasmic tail CT (green box), S1/S2 and S2' cleavage site, presence of D614G, P681H/R mutation **b.** Surface expressed spike protein binding to soluble-hACE2

was analyzed by expressing the spike of variants and mutants in HEK 293T cells and 36 h post transfection incubated with soluble-hACE2 and analyzed by flow cytometry. Each value represents a single mean value of two repeated experiments. Statistical significance was determined using the one-way ANOVA test ($p < 0.05$), where *** and ** $p < 0.05$ is significant. **c.** Detection of spike protein cleavage in different pseudoviruses at 24h and 48h post transfection by Western blot analysis, p24 was kept as loading control.

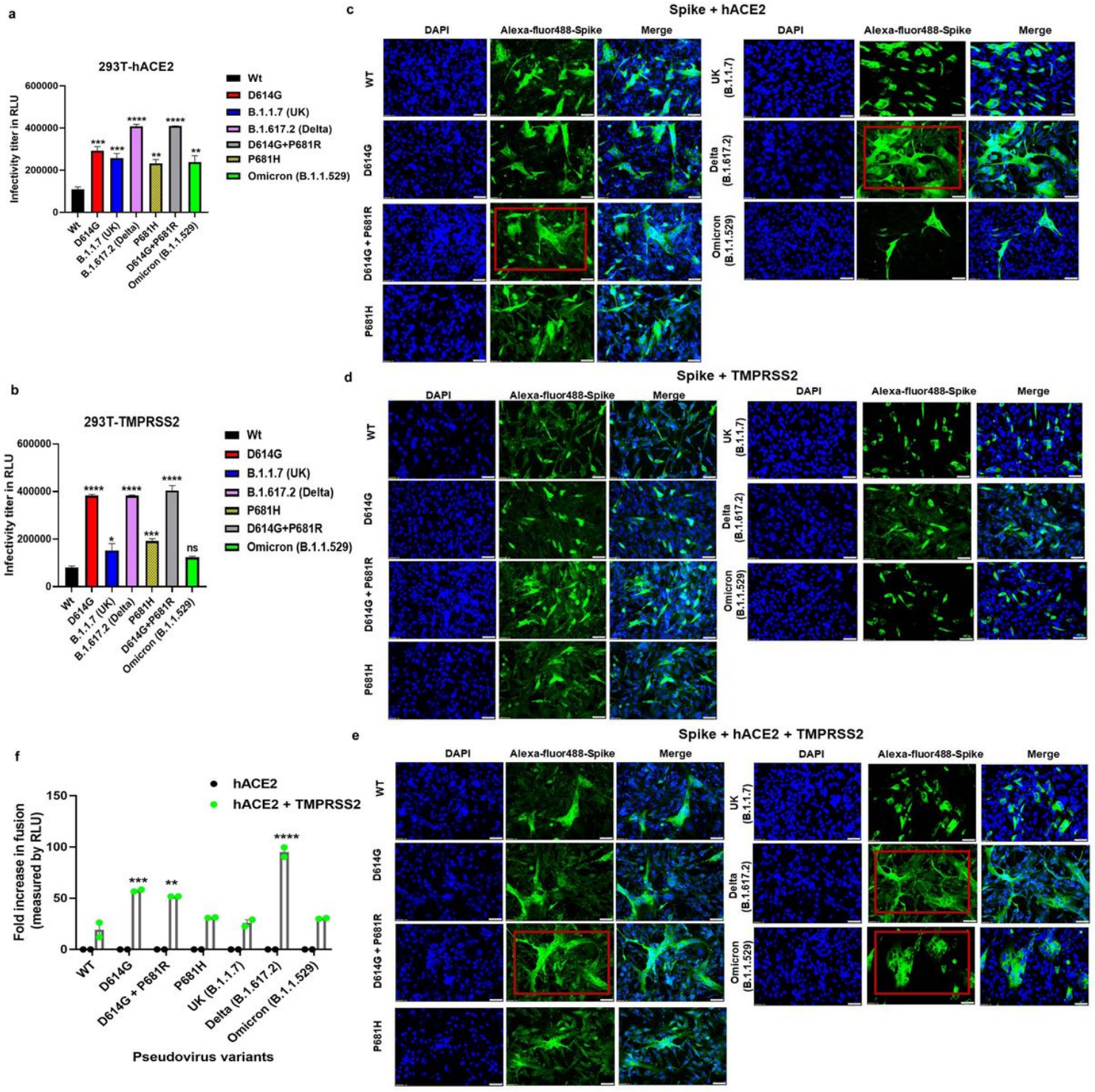

Figure 2

Infectivity titer and fusion of pseudovirus variants and mutants: a. Pseudoviruses are produced in HEK-293T cells and infectivity was measured in 293T over-expressing hACE2 cell line (NR52511, BEI resources, USA) **b.** 293T over expressed TMPRSS2 (293T cells transfected with TMPRSS2 plasmid and harvested 24h post transfection and used in the assay) were infected with pseudoviruses and infectivity titer was measured 48 h post infection as relative luciferase units (RLU). Each bar represents mean of three experiments in duplicate. **c.** Fusion and syncytial formation as shown in BHK-21 cells; spike variant plasmids and hACE2 plasmid are co transfected in BHK-21 cells and probed with anti-Spike mouse polyclonal sera (1:200) and Alexa-Fluor 488-labeled anti-mouse antibody (green) (1:1000) after 36-hour post transfection. **d.** Spike variant plasmids and TMPRSS2 plasmid are co transfected in BHK-21 cells and fusion formation was shown by immunofluorescence **e.** Spike variant plasmids, hACE2, TMPRSS2 plasmids are co transfected in BHK-21 cells. The images were taken in Olympus fluorescence microscope. The experiments were repeated three times. The nuclei were stained with 4',6-diamidino-2-phenylindole (DAPI, blue); scale bar: 50 μm and magnification 20x. **f.** Quantitative fusion assay in presence of hACE2 or hACE2+TMPRSS2 as measured by RLU. Data shown are the averages and standard error of the mean (SEM) of three experiments in duplicates. Statistical significance was determined using the one-way ANOVA test where ($p < 0.05$), *P <0.05, **P<0.01, ***P<0.001, ****P<0.0001 considered significant and $p>0.05$ as non-significant (ns).

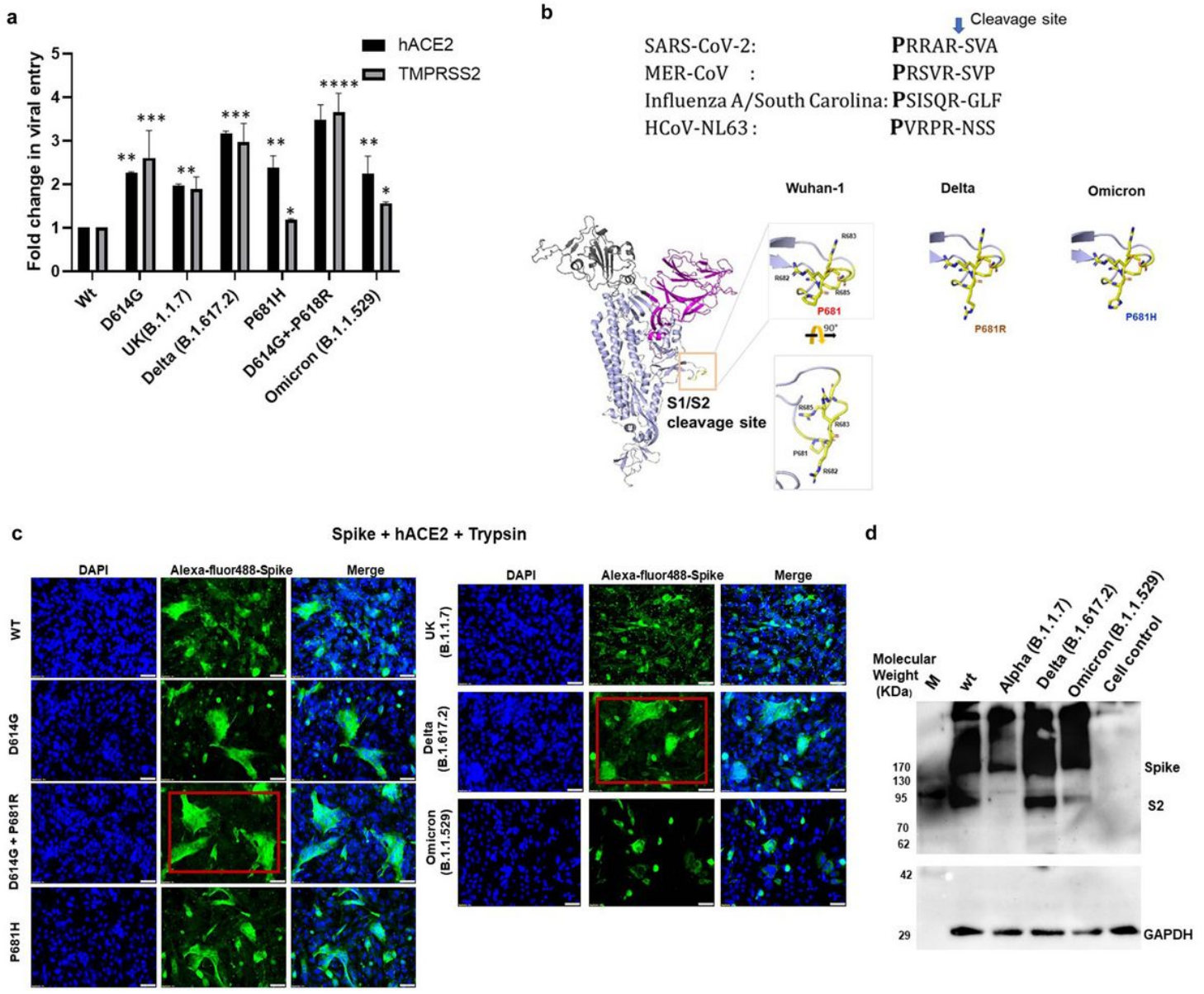

Figure 3

Pseudovirus variants cell tropism to ACE2 and TMPRSS2 and effect of trypsin in fusion and cleavage. a) Pseudovirus entry was measured in 293T cells transfected with either hACE2 or TMPRSS2 plasmid. 36h post transfection, 293T cells expressing hACE2 or TMPRSS2 were infected with variants and synthetic pseudoviruses and relative luciferase titers were measured 48-hour post transfection. The experiments were repeated two times in triplicates. **b.** Cleavage site sequences and the overall cartoon representation of a monomer of the ectodomain of SARS-CoV-2 spike glycoprotein in prefusion conformation. The RBD is shown in gray, the NTD in purple and the S2 domain is shown in light blue color. The furin cleavage site at the junction of S1 and S2 is shown in yellow. This region is a flexible loop like structure and exposed in the prefusion conformation for easy accessibility to the proteases. The cleavage site is rich in Arg residue. A magnified view of the cleavage side with the Arg residues showed as sticks. **c.** Fusion and syncytial formation in BHK-21 cells co transfected with spike variant and hACE2 plasmids in presence of trypsin **d**. Cleavage of ancestral, Alpha, Delta and Omicron variants spike protein in presence of trypsin as

analysed by Western blot. Data shown are the averages and standard error of the mean (SEM) of three experiments in duplicates. Statistical significance was determined using the one-way ANOVA test where ($p < 0.05$), *P <0.05, **P<0.01, ***P<0.001, ****P<0.0001 considered significant.

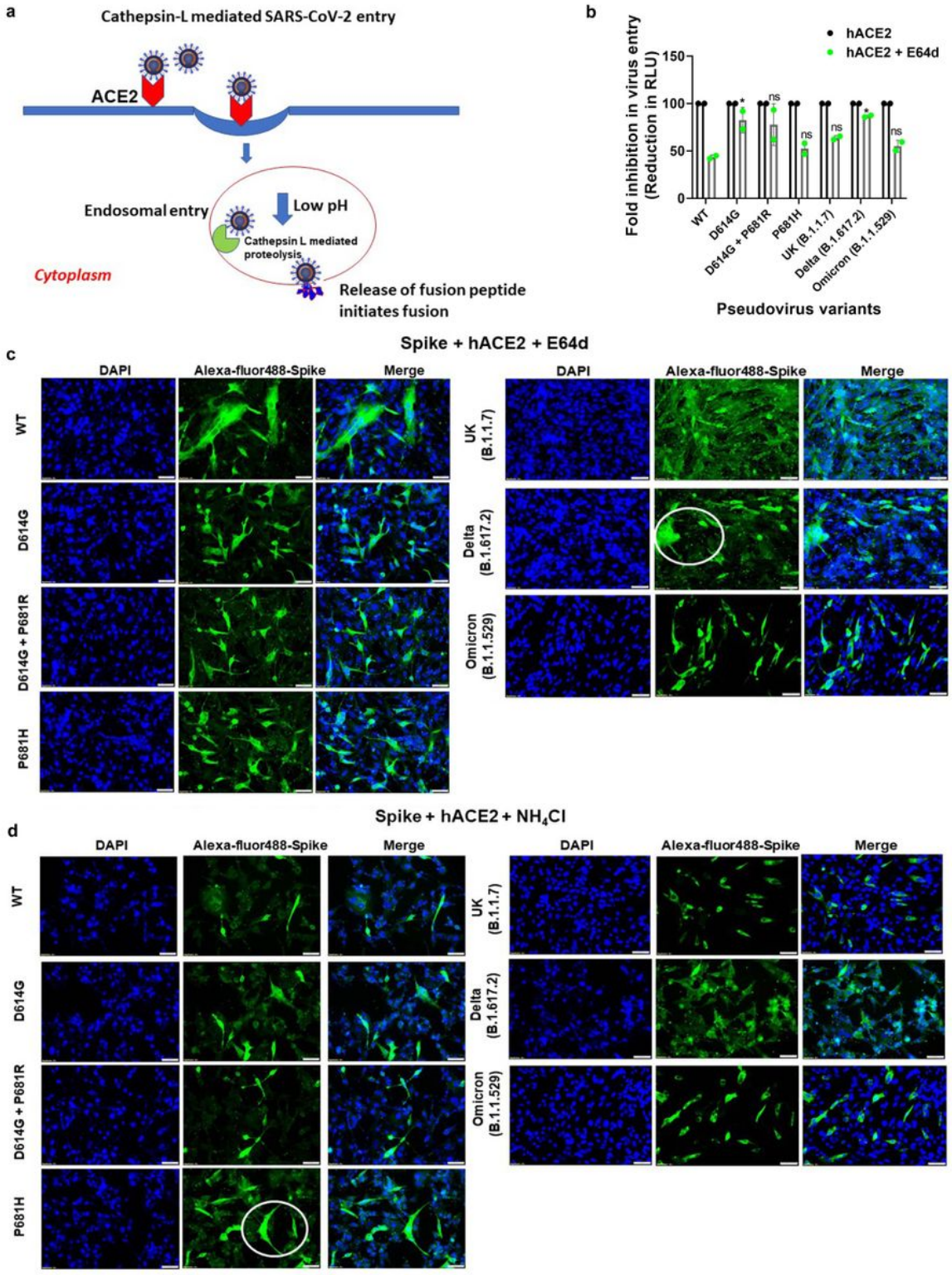

Figure 4

Analysis of variants entry and fusion in presence of Cathepsin L inhibitors. a. Schematic representing ACE2-mediated endosomal entry and activation by Cathepsin -L proteases in endosome **b**. Pseudoviruses entry in absence or presence of Cathepsin L inhibitor E64d. The experiments were repeated three times in duplicates **c.** Fusion of variants spike proteins co-expressed with ACE2 in presence of E64d in BHK-21 cells. **d.** Fusion of variants spike proteins co-expressed with ACE2 in presence of NH_4Cl in BHK-21 cells. The spike protein was probed with primary anti-Spike mouse polyclonal sera (1:200) (ancestral spike protein) and secondary antibody Alexa-Fluor 488-labeled anti-mouse antibody (green) (1:1000) after 36-hour post transfection. The images were taken in Olympus fluorescence microscope. The experiments were repeated three times. The nuclei were stained with 4',6-diamidino-2-phenylindole (DAPI, blue); scale bar: 50 μm and magnification 20x. Data shown are the averages and standard error of the mean (SEM) of three experiments in duplicates. Statistical significance was determined using the one-way ANOVA test where ($p < 0.05$), *P <0.05, considered significant and p>0.05 as non-significant (ns).

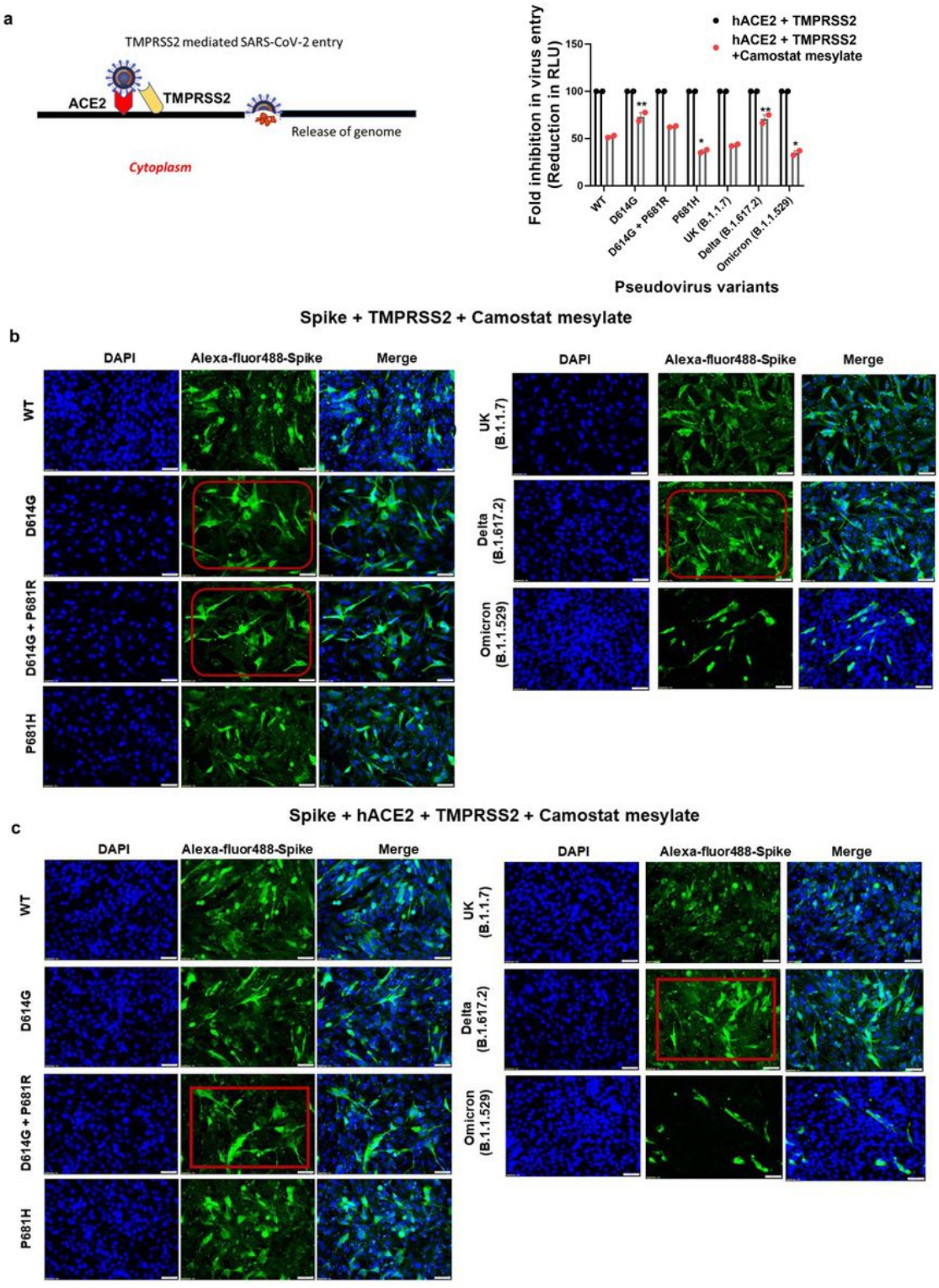

Figure 5

Analysis of variants entry and fusion in presence of serine protease TMPRSS2 inhibitor Camostat mesylate. a. Pseudoviruses entry in absence or presence of Camostat mesylate inhibitor when spike co-expressed along with hACE2 and TMPRSS2. The experiments were repeated three times in duplicates c. Fusion of variants spike proteins co-expressed with TMPRSS2 in presence of Camostat mesylate in BHK-21 cells. d. Fusion of variants spike proteins co-expressed with hACE2 and TMPRSS2 in presence of

Camostat mesylate in BHK-21 cells. The spike protein was probed with primary anti-Spike mouse polyclonal sera (1:200) (ancestral spike protein) and secondary antibody Alexa-Fluor 488-labeled anti-mouse antibody (green) (1:1000) after 36-hour post transfection. The images were taken in Olympus fluorescence microscope. The experiments were repeated three times. The nuclei were stained with 4',6-diamidino-2-phenylindole (DAPI, blue); scale bar: 50 μm and magnification 20x. Data shown are the averages and standard error of the mean (SEM) of three experiments in duplicates. Statistical significance was determined using the one-way ANOVA test where ($p < 0.05$), *P <0.05, **P<0.01 considered significant and $p>0.05$ as non-significant (ns).

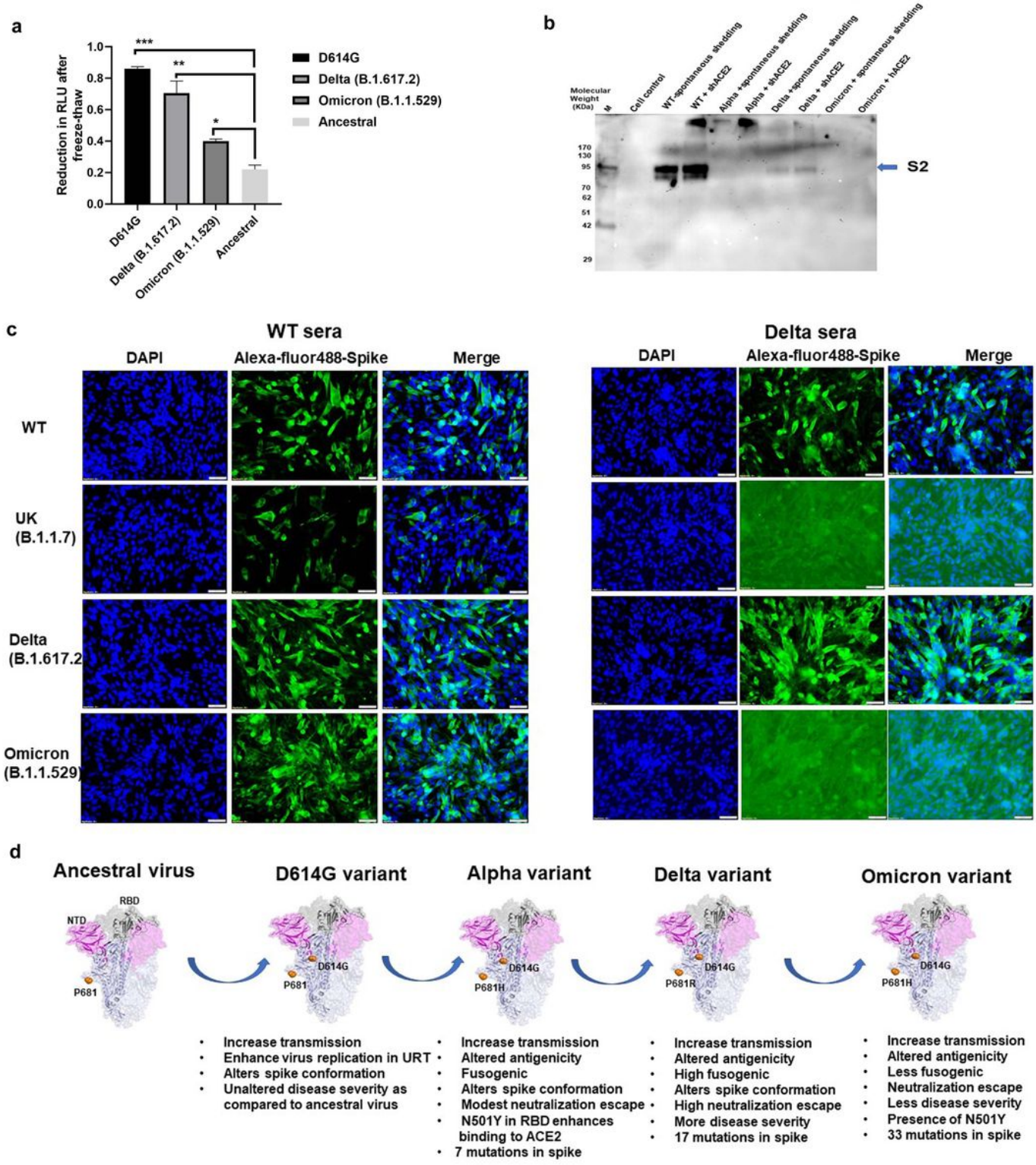

Figure 6

Stability, shedding, antigenicity and characteristics of variants w.r.t D614G and P681R/H mutation. a. Measurement of infectivity titers of ancestral, D614G, Delta and Omicron pseudoviruses in 293T-hACE2 cell lines after two times freeze-thaw. The experiment was repeated three times in duplicates. **b.** Assessment of soluble-hACE2 induced and spontaneous shedding of S1 domain as measured by Western blot. **c.** Cross reactivity of Omicron, Alpha spike to anti-Delta RBD polyclonal mouse sera as

measured by immunofluorescence. Briefly, spike protein was transfected in BHK-21 cell line and 36h post transfection the cells were fixed and probed with anti-RBD (ancestral Wuhan-1) or anti-Delta RBD polyclonal mouse sera (1:200 dilution) and secondary antibody Alexa-Fluor 488-labeled anti-mouse antibody (green) (1:1000 dilution). The images were taken in Olympus fluorescence microscope. The experiments were repeated two times. The nuclei were stained with 4',6-diamidino-2-phenylindole (DAPI, blue); scale bar: 50 μm and magnification 20x. **d.** Structural modeling of spike protein was created by using the PYMOL software. Pink represents N terminal domain and grey RBD domain, orange dots, D614G and P681H/R mutations. The evolution of virus and variants characteristics were schematically represented. Data shown are the averages and standard error of the mean (SEM) of three experiments in duplicates. Statistical significance was determined using the one-way ANOVA test where ($p < 0.05$), *P <0.05, **P<0.01, ***P<0.001considered significant.

Supplementary Files

This is a list of supplementary files associated with this preprint. Click to download.

- SupplementaryFig.1.tif
- SupplementaryFig.2.tif
- SupplementaryFig.3.tif
- SupplementaryInformation.docx